Supplemental note of "Intrinsically disordered regions direct transcription factor *in-vivo* binding specificity"

Our results suggest that intrinsically disordered regions (IDRs) direct transcription factors (TFs) to their target promoters. This is supported by the DNA binding profiles of intact and mutant TFs which we characterized in the study. Particularly informative are the following three main results: (1) The removal (or swapping) of the non-DNA binding domain (non-DBD) changes the TF binding pattern, (2) a TF mutant containing only the non-DBD can still bind a large fraction of promoters bound by the intact TF and (3) truncating the non-DBD leads to a gradual loss of binding specificity. **Our key findings therefore depend on the ability to define the DNA binding profiles of the intact TFs and of their mutants lacking large segments of their sequence.** In all of the experiments presented in the main text, we used the ChEC-seq method (Zentner et al., 2015). We routinely use this method in the lab, as we found it to be of high resolution and sensitivity. Still, this method is relatively new and used less frequently than the traditional co-immunoprecipitation (co-IP) approach. **In this supplementary note, we support our conclusions by comparing the ChEC-seq results to binding profiles derived by two additional methods: ChIP-seq and CUT&Tag.** In this analysis, we further support the ChEC-seq profiles of the intact and mutant TFs by showing that they all bind transcriptionally regulated and motif-containing promoters.

A. ChEC-seq binding profiles are supported by ChIP-seq and CUT&Tag:

We performed a side-by-side comparison of three binding assays: ChIP-seq, CUT&Tag and ChEC-seq. ChEC-seq and CUT&Tag replace fixation and co-IP with DNA cleavage around the TF binding sites. In ChEC-seq, DNA is cleaved by an MNase that is endogenously fused to the TF of interest (Zentner et al., 2015). In CUT&Tag, DNA in the proximity of the TF is cleaved by an antibody-conjugated Tn5 following relatively long (>24 hours) pre-processing (Kaya-Okur et al., 2019). The ChEC-seq approach therefore presents two key advantages – (1) not relying on anti-bodies, and (2) rapid DNA cleavage which occurs almost immediately after cell harvesting.

Despite their large methodological differences, the ChEC-seq profiles of Msn2 and Yap1 are in good agreements with the respective ChIP-seq and CUT&Tag profiles, reaching a correlation of r = 0.78 (Pearson) when comparing the Msn2 promoter selection defined by ChEC-seq and CUT&Tag (Figure SN1A; note also agreement of motif binding preferences Figure SN1B). In comparison, correlations between previously reported ChIP-based profiles are significantly lower (Pearson's r < 0.25, Figure SN1A; Harbison et al., 2004; Kuang et al., 2017; Tan et al., 2008; Venters et al., 2011). Next, we used these profiles to control for the possibility that the high correlation in promoter selection between the intact TF and its mutant lacking the DBD (Pearson's r = ~0.7) results from ChEC-seq-specific biases. To this end, we compared the binding of the DBD deleted mutant (as derived by ChEC-seq) to that of the wild-type protein, as derived by ChIP-seq and CUT&Tag. Indeed, **both ChIP-seq and CUT&Tag profiles were similar to the ChEC-seq profiles of the DBD-deleted mutants** (non-DBDs; Figure SN1 C-D). Therefore, these two independent binding assays support the ChEC-seq profiles of Msn2 and Yap1, and verify that the high similarity between the profiles of the non-DBD and intact TFs do not result from ChEC-seq specific biases.

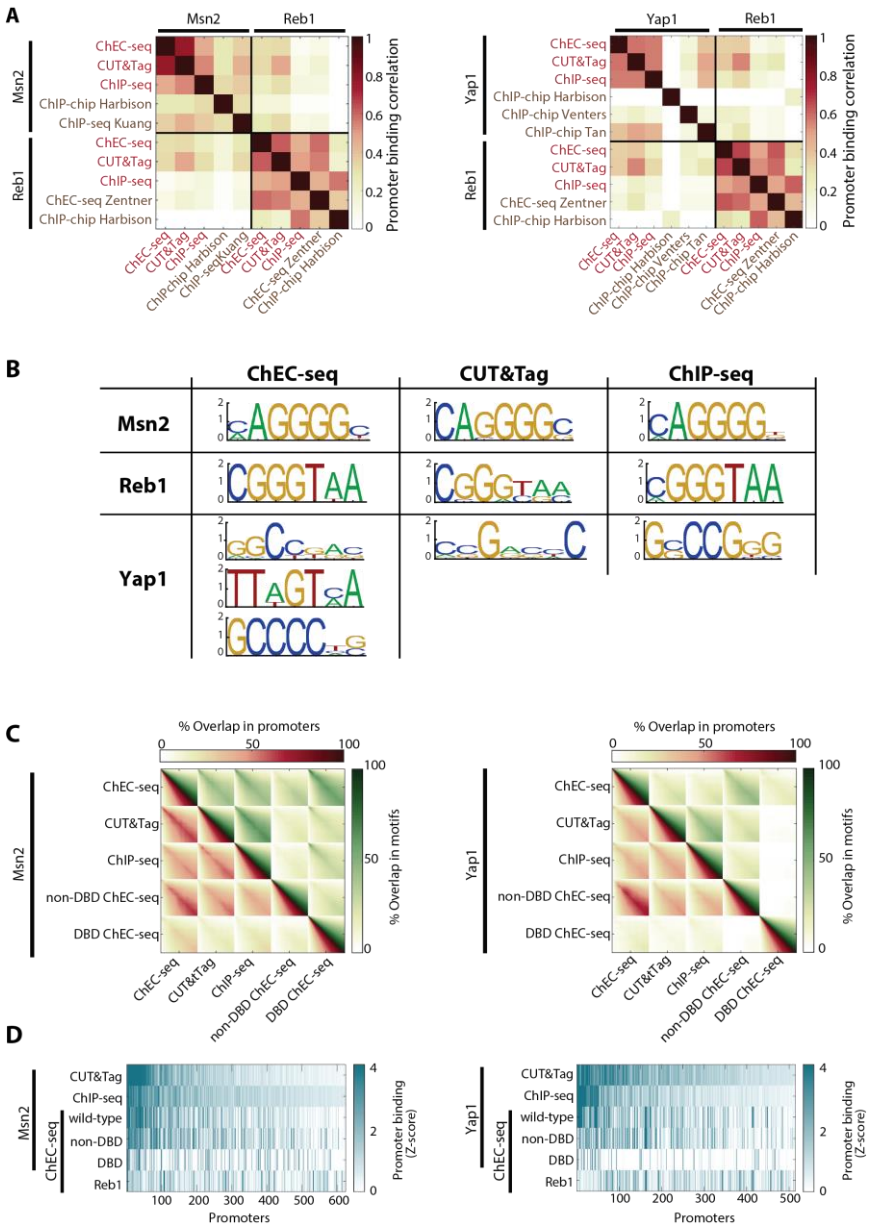

Figure SN1: Similarity of ChEC-seq, ChIP-seq and CUT&Tag binding profiles.

(A) *Patterns of promoter binding:* Shown are the genome-wide correlations in promoter binding of Msn2 (left panel) and Yap1 (right panel), as detected by the different methods. Included in this analysis are profiles generated for this study (ChEC-seq, CUT&Tag and ChIP-seq, indicated in red), and profiles reported by others (Harbison et al., 2004; Kuang et al., 2017; Tan et al., 2008; Venters et al., 2011; Zentner et al., 2015; indicated by brown color). The TF Reb1 is shown as a control.

(B) *Preferred sequence motif:* Preferred binding motifs were defined as described in main text (see methods). Shown are the respective Probability weight matrices (PWMs) obtained from the indicated TF profiles in all three methods.

(C) *The ChEC-seq non-DBD profiles correlate with the intact-TF profiles measured in different assays:* Pearson correlations between the ChEC-seq non-DBD profile and the wild-type profiles defined by ChEC-seq, ChIP-seq and CUT&Tag are, respectively, 0.72, 0.43 and 0.59 for Msn2, and 0.69, 0.3 and 0.44 for Yap1. To quantify this similarity, we measured the overlap between top-bound promoters (red, lower triangle), or top-preferred 7-mers (green, upper triangle). Since such overlap, defined as the number of common promoters normalized by the size of the larger group, depends on a threshold, we scanned across a range of thresholds (ranging from 5 to 500), gradually increasing the number of selected promoters/motifs from each dataset. Each square displays this range of overlap values as a function of the number of promoters/motifs selected from each of the indicated datasets. Overlap values are shown by color. The diagonal in each square corresponds to cases where equal-size groups are compared.

(D) *The non-DBDs bind to promoters detected as WT-bound in other methods:* Columns represent all promoters showing high binding signal in both CUT&Tag and ChIP-seq. Color indicates binding strength (in Z-score; median values of all repeats) to each promoter in the indicated profiles. Promoters are ordered by the mean binding signal of the ChIP-seq and CUT&Tag profiles.

B. ChIP-seq and CUT&Tag are not sensitive enough for measuring the binding profiles of the mutant TFs:

We also tried to measure the binding profiles of the DBD and non-DBD mutants using ChIP-seq and CUT&Tag. However, in our hands, neither method was sensitive enough to detect DNA binding of these mutants. This lack of sensitivity was judged by the following three indicators, expected to apply to profiles that represent real TF binding : (1) Preferential binding to known binding motifs (or to promoters containing these motifs), (2) preferential binding to transcriptionally regulated promoters, and (3) low similarity with same-method profiles of other TFs. As we detail below, the ChEC-seq non-DBD and DBD profiles complied with all these conditions, while the ChIP-seq and CUT&Tag profiles complied with none.

B1. Evaluating binding profiles by preferential localization at known motifs:

The intact TFs should localize to their *in-vitro* preferred motifs. When examining the Msn2 preference for binding the AGGGG motif, we noted a large difference between the three methods: ***The ChEC-seq signal was distributed over a wider dynamic range, and thereby detected more bound sites, as compared to ChIP-seq and CUT&Tag*** (Figure SN2A-B). Furthermore, in the case of Yap1 ***only ChEC-seq detected the biased localization to its preferred in-vitro motif*** (Figure SN2A-D). Neither ChIP-seq nor CUT&Tag showed this expected bias. As we discuss below (Part C), detecting the Yap1 motif preference requires increased sensitivity due to competing processes contributing to its within-promoter localization. Indeed, previous genomic analysis identified the preferential *in-vivo* localization of Yap1 to its *in-vitro motif* only when including properties such as evolutionary conservation or *in-vitro* binding scores (MacIsaac et al., 2006). The fact that ChEC-seq captures the Yap1 preference for binding this *in-vitro* defined motif emphasizes the sensitivity of this method.

The DBD-only mutants should also localize to their preferred *in-vitro* motifs. Indeed, the ChEC-seq DBD profiles of both Msn2 and Yap1 showed this preference, presenting a localization bias that was in fact stronger than that of the intact TF: the DBD localized to a narrower region around the motif, and gave a higher signal when averaged over all motif occurrences. By contrast, neither the ChIP-seq nor CUT&Tag DBD profiles showed any preference for localizing at their preferred *in-vitro* motif (Figure SN2A-D).

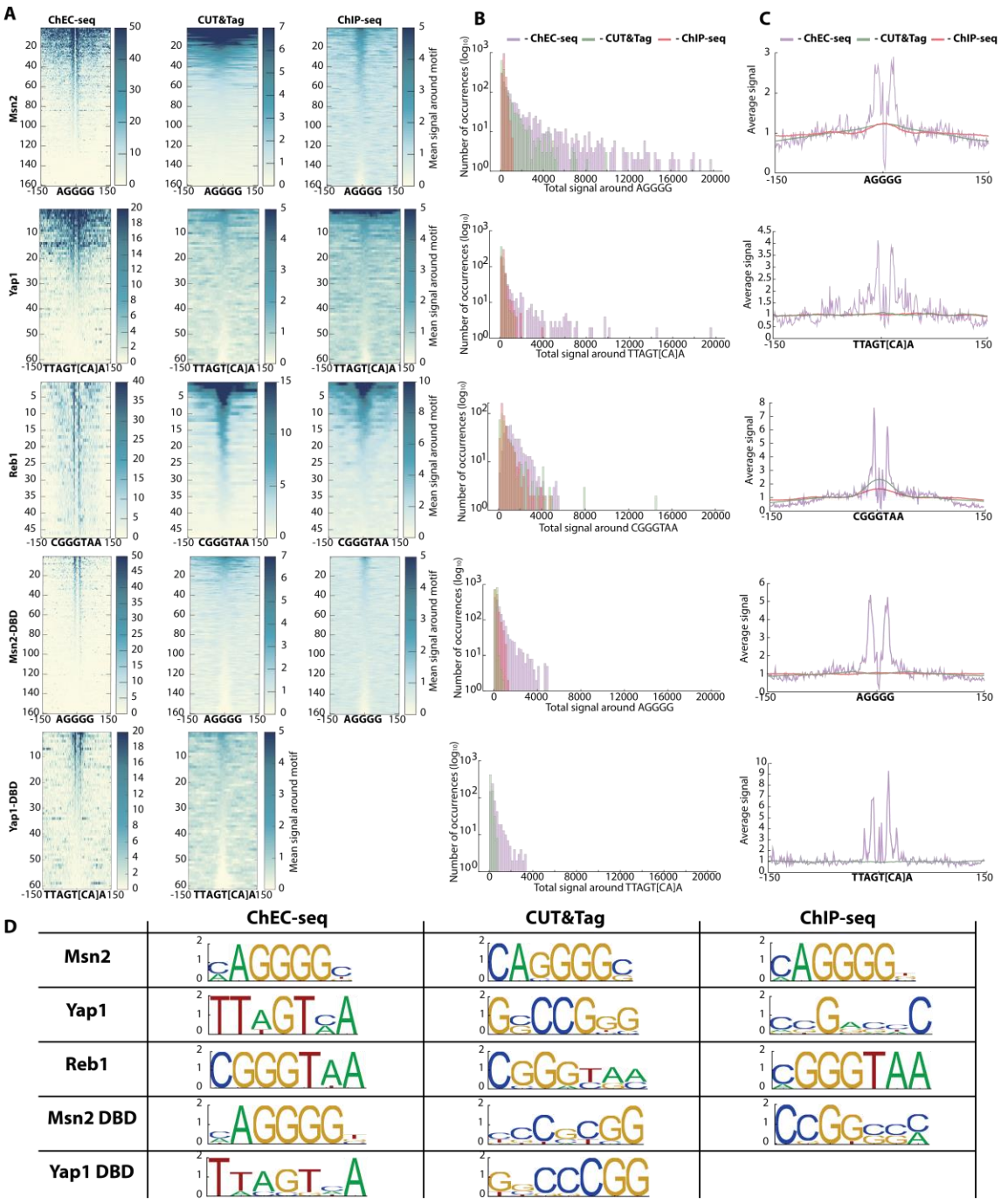

Figure SN2: ChEC-seq profiles best captures motif binding preferences.

(A-C) *Binding around in-vitro preferred motifs:* Shown in **(A)** is the binding of the indicated TFs at the 300 base-pairs surrounding the indicated motif. All genomic occurrences in promoter sequences were divided into bins based on binding strength, each bin containing 10 occurrences. The mean signal per bin was calculated and bins were ordered based the average binding intensity of the 30-bps surrounding the motif. The distribution of intensities at motif sites are shown in **(B)**, as well as the average signal over all presented occurrences, normalized by the median signal within the same 300 base-pair window **(C)**. Note the higher dynamic range of the ChEC-seq profiles, suggesting a better signal to noise ratio. Note also that the ChEC-seq DBD profile localizes to a narrower region around the motif, while the wild-type profile extends more broadly in these sites, consistent with the proposed IDR-directed recognition.

(D) *Preferred sequence motif:* Preferred motifs were defined as described in the Methods section of the main text. Shown are the respective PWMs obtained from all indicated profiles. For the Yap1 ChEC-seq profile, shown is the *in-vitro* motif cluster, which corresponds to the DBD preferred motif. Note that, when testing DBD only mutants, only ChEC-seq profiles retrieve the known *in-vitro* motifs of Msn2 and Yap1. When testing the full proteins, ChIP-seq and CUT&Tag retrieve the Msn2 and Reb1 canonical binding sequences, but not that of Yap1.

The TF mutant that lacks the DBD (non-DBD) is not expected to localize to the wild-type preferred *in-vitro* motif, as was indeed the case. We therefore validated the non-DBD profiles by looking at broader regions surrounding the small binding motif. Specifically, we asked whether the non-DBD mutants show preferential binding to promoters containing the intact TF preferred motif. Indeed, the Msn2 non-DBD profile, measured by ChEC-seq, showed a strong preference for binding AGGGG-containing promoters (Figure SN3A-C). By contrast, neither the ChIP-seq nor CUT&Tag non-DBD profiles showed such enrichment (Figure SN3C). Yap1 did not show such preference in any of the methods, and is discussed below.

Taken together, we concluded that, ChEC-seq derived profiles capture the preference of the mutant TFs for localizing to their expected binding motif, or to promoters containing this motif. By contrast, profiles derived by the two other methods did not show this expected localization, suggesting that they are not sensitive enough to capture the binding of these mutants.

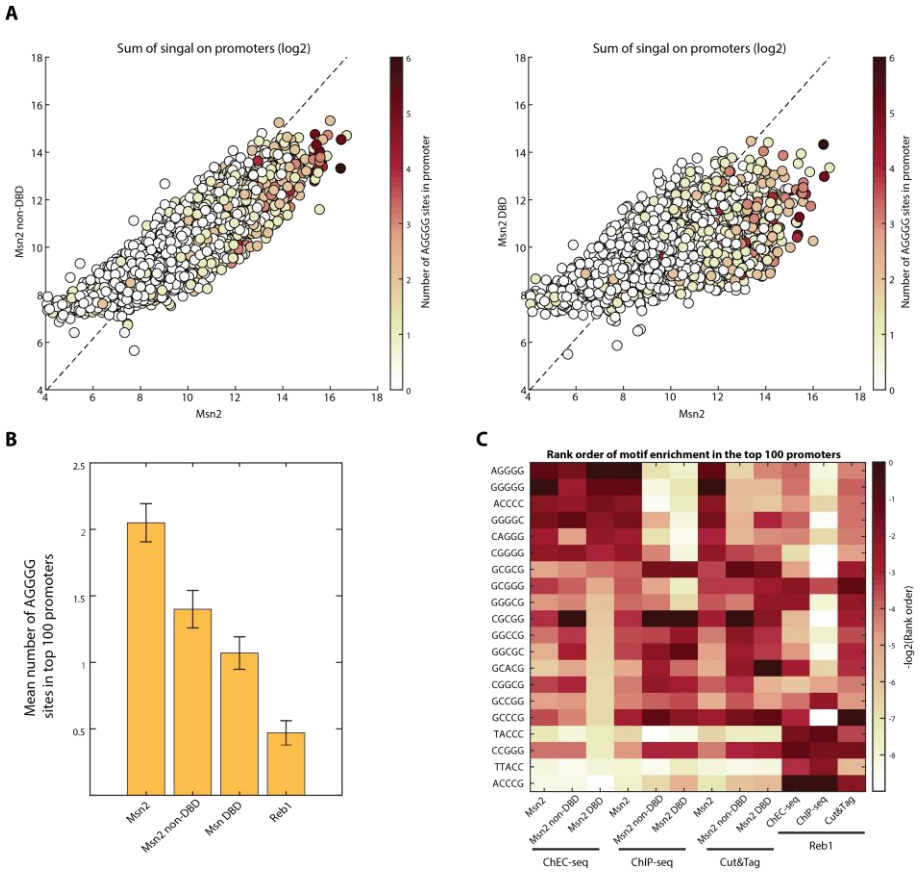

Figure SN3: The ChEC-seq Msn2 non-DBD binds preferentially to AGGGG-containing promoters.
(A) *Similarity between Msn2 and its non-DBD profile includes binding to AGGGG-containing promoters:* The figure on the left compares the promoter binding strength of Msn2 and its non-DBD. Each dot represents a promoter, the color of each dot indicates the number of AGGGG sites present in this promoter. Comparison with the binding of the DBD mutant is also shown (right).
(B) *AGGGG is found within top-bound non-DBD promoters:* Shown is the average number of AGGGG occurrences within the top 100 bound-promoters in each of the indicated datasets. Error bars represent the standard error of the mean (SEM).
(C) *AGGGG is enriched within promoters bound by the ChEC-seq non-DBD profile but not in profiles generated by other methods:* All 5-mers were ordered based on their enrichment within the top-100 bound promoters (See Methods section). This analysis was repeated for all indicated datasets. Shown is the rank-order of the indicated motifs in each dataset. Included here are all motifs ranked among the top 3 in at least one dataset. Motifs were ordered based on their rank in the DBD ChEC-seq profile. Note the high ranking of the AGGGG motif and of similar sequences in the non-DBD ChEC-seq profile.

B2. Evaluating binding profiles by preference for binding regulated genes:

As another way to evaluate the different binding profiles, we examined whether they show preference for binding promoters that are transcriptionally regulated by the respective TFs. To this end, we defined the lists of expression target genes of both Msn2 and Yap1. We recently characterized at details the Msn2/4-dependnet transcriptional response to an array of stresses and used this data to define the top 72 Msn2 regulated genes (methods). For Yap1, we tested several datasets and found low reproducibility between them. We decided to use a list of target genes defined in a previous study performed in Yap1-inducing conditions (Tan et al., 2008).

In the case of the intact TFs, profiles derived using all three methods showed the expected enrichment of binding regulated promoters. For Msn2, >50% of regulated promoters were among the 100 top-bound promoters detected by ChEC-seq, and >40% among the top bound promoters in the CUT&Tag and ChIP-seq profiles (Figure SN4A). For Yap1, the fraction of regulated promoters that were bound in any of the assays was lower, but still showed significant enrichment (The highest overlap was derived by the ChEC-seq profile - 16% of the top bound promoters). The ChEC-seq DBD and non-DBD profiles of both Msn2 and Yap1 showed significant enrichment for binding regulated promoters. Such enrichment is not detected when examining profiles generated by neither ChIP-seq nor CUT&Tag (Figure SN4A). Therefore, consistent with the motif analysis above, these results further indicate that ChEC-seq is the only method sensitive enough to capture the binding profiles of the DBD and non-DBD TF mutants.

B3. Evaluating binding profiles by comparing same-method vs. same-mutant similarity:

Each profile reports on binding signals, superimposed on method-specific biases. Low-signal profiles will therefore be similar to other low-signal profiles generated by the same method. This appears to be the case of the Msn2 ChIP-seq and CUT&Tag mutant profiles: The correlation between the non-DBD profiles is low (Pearson's r = 0.16), but the non-DBDs in both methods are highly correlated with the same-method DBD (Pearson's r = 0.45 for CUT&Tag and 0.87 for ChIP-seq; Figure SN4B). By contrast, the ChEC-seq non-DBD profile showed little correlation with the DBD from the same method but was similar to the intact-TF profiles derived by all three methods, supporting its validity (Figure SN4B-C).

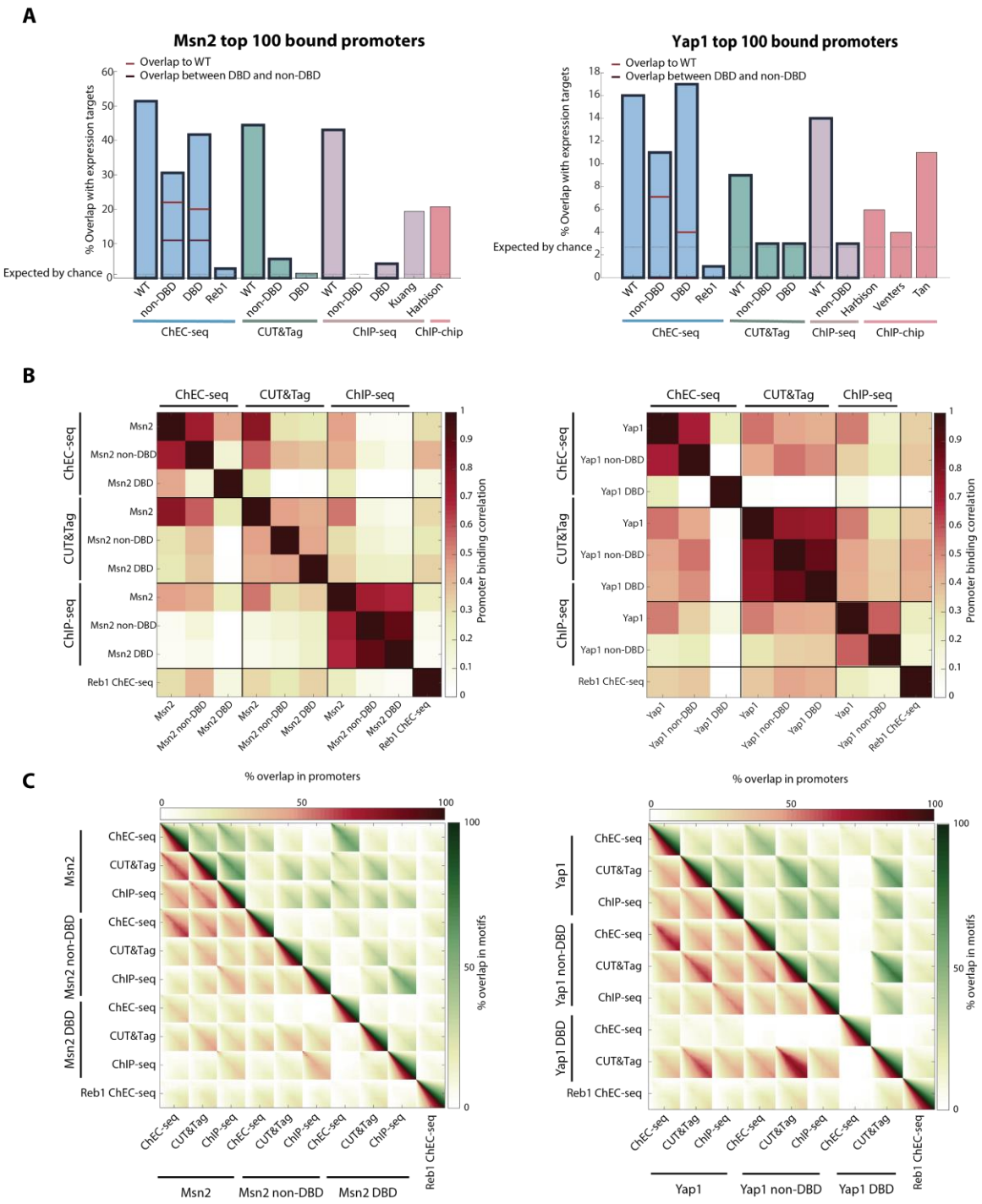

Figure SN4: Evaluating the quality of the mutant profiles.

(A) *Overlap between expression targets and binding data:* Expression targets of Msn2 (left) and Yap1 (right) were defined based on transcriptional changes in the respective mutants (See Methods section). The fraction of regulated targets within the top-100 bound promoters is shown for datasets generated for this study (bold outline) and previously published studies (Harbison et al., 2004; Kuang et al., 2017; Tan et al., 2008; Venters et al., 2011). Note the high overlap with expression targets of mutant profiles generated by ChEC-seq, compared to the low overlap measured by both ChIP-seq and CUT&Tag.

(B-C) *Same-TF vs. same-method similarity:* Shown are correlations **(B)** and overlaps **(C)** between the indicated datasets. The overlap is defined as in Figure SN1C above. Note the high within method similarity between the non-DBD and DBD profiles detected by ChIP-seq and CUT&Tag, in comparison to the low similarity between the ChEC-seq non-DBD profiles and that of the DBDs.

C. Characteristics of the Yap1 ChEC-seq profile:

Our analysis above supports the validity of the ChEC-seq derived profiles we reported. Still, we were puzzled by the fact that the Yap1 non-DBD, whose binding profile was highly correlated with that of the intact TF, did not show preferential localization to promoters containing its known *in-vitro* preferred motif, and therefore decided to follow up more closely on the determinants of Yap1 binding. As discussed above, preferential binding of Yap1 to its *in-vitro* motif (TTAGT[CA]A) was recognized (only) by the ChEC-seq profiles of the intact TF and its DBD, but not by profiles generated by ChIP-seq or CUT&Tag. This motif is the most-preferred 7-mer bound by the DBD. However, it is ranked only at the 8th position in the Yap1 profile. In this later case, the most enriched motifs correspond to the *in-vitro* binding preferences of Skn7, a Yap1-interacting TF (Mulford and Fassler, 2011). We initially hypothesized that Skn7 recruits Yap1 to these promoters. However, as we described in the main text, **deletion of Skn7 abolished the Yap1 localization to Skn7 sites, but had a minor effect on the overall Yap1 promoter binding**.

We used our motif analysis to better clarify the respective contributions of the Yap1 DBD and Skn7 to the Yap1 localization to, and within, promoters. As we describe in the manuscript, we defined the Yap1 motif preference by assembling the top 50 enriched 7-mers. Visual inspection suggested that these sequences correspond to several consensus motifs, and we therefore clustered the selected 7-mers into three groups based on their nucleotide content (see Methods section - "Motif sequence clustering" in the main text). Of the three consensus motifs defined by this analysis, two corresponded, respectively, to the known Yap1 and Skn7 binding motifs. The third cluster contained a large number of GC-rich motifs, as did the Skn7-cluster, but we could not interpret its inferred consensus. **Below we show that this third cluster is functionally equivalent to the Skn7 cluster.**

To understand whether the motif-clusters are indicative of function, **we used these clusters to classify promoters.** Specifically, we assigned promoters to one of the three classes based on the sequences found in the proximity of the Yap1-binding peaks found in each promoter (Figure SN5A and Methods section "Yap1/Skn7 promoter class definition"). A total of 345 promoters were assigned to one of the three clusters, 56% of which were DBD-dominated. We next tested this classification, as follows:

a. *The DBD only mutant localizes to DBD-classified promoters:* We compared promoter binding by the DBD-only mutant to that of the intact Yap1, color-coding each promoter by its class association (Figure SN5B). As can be appreciated, the DBD-only mutant localized almost exclusively to DBD-classified promoters. Of note, the DBD-only mutant gained binding to DBD-classified promoters that were poorly bound by the intact Yap1, while showing reduced binding to the two other promoter classes.
b. *Skn7 binds preferentially to promoters of the "Skn7" and "Unknown" classes*: As described in the manuscript, the promoter selection of Yap1 and Skn7 is highly correlated (Pearson's r = 0.57). To examine whether Skn7 binds to Skn7-classified promoters, we compared the binding strength of Skn7 and Yap1 to the different promoters, color-coding each promoter by its class association (Figure SN5C). As can be appreciated, Skn7 binds strongly to promoters classified to the Skn7 or unknown class, while showing little binding to DBD-classified promoters.
c. *Skn7 deletion causes a minor reduction of the Yap1 binding to promoters of the Skn7 and 'unknown' classes:* As discussed in the manuscript, deletion of Skn7 had little effect on the overall promoter selection of Yap1 (Pearson's r = 0.91). Still, when considering our

classification, we observe a minor, but clear reduction of the Yap1 binding to the Skn7 and the unknown-classified promoters (Figure SN5D).

d. *ChIP-seq and CUT&Tag detect Yap1 binding to promoters of all classes*: Finally, we verified that the Yap1 binding to Skn7-associated promoters is not specific to ChEC-seq but is detected also by other methods (Figure SN5E).

Together, these results support the following model:

1. Yap1 is directed to selected promoters by its non-DBD.
2. Within this subset of selected promoters, binding of Yap1 is stabilized in (at least) two ways:
    a. Binding of the Yap1 DBD to its *in-vitro* preferred motif
    b. Association with Skn7.

Going back to the non-DBD profile, this model provided several testable predictions:

a. *DBD deletion increases correlation with Skn7:* If the DBD stabilizes the Yap1 binding at DBD, but not at Skn7-classified promoters, its deletion should increase the correlation with Skn7. As we show, Skn7 binding correlates more tightly with the non-DBD than with the intact Yap1 (Figure SN5F).

b. *DBD deletion specifically reduces binding to DBD-classified promoters:* If the DBD is required for stabilizing Yap1 specifically on DBD-classified promoters, then the non-DBD should show reduced binding preferentially at these promoters. We verified that this is indeed the case by comparing promoter binding by the DBD deleted mutant and the intact Yap1, color-coding each promoter by its class association (Figure SN5G).

c. *Skn7 deletion partially compensates for the loss of non-DBD binding to DBD-classified promoters:* This prediction, which follows from the fact that both stabilizing mechanisms are deficient, is indeed supported by the data (Figure SN5H).

Therefore, the ChEC-seq profile of the Yap1 non-DBD complies with the prediction of the binding model derived above, supporting both the model and the validity of the profile.

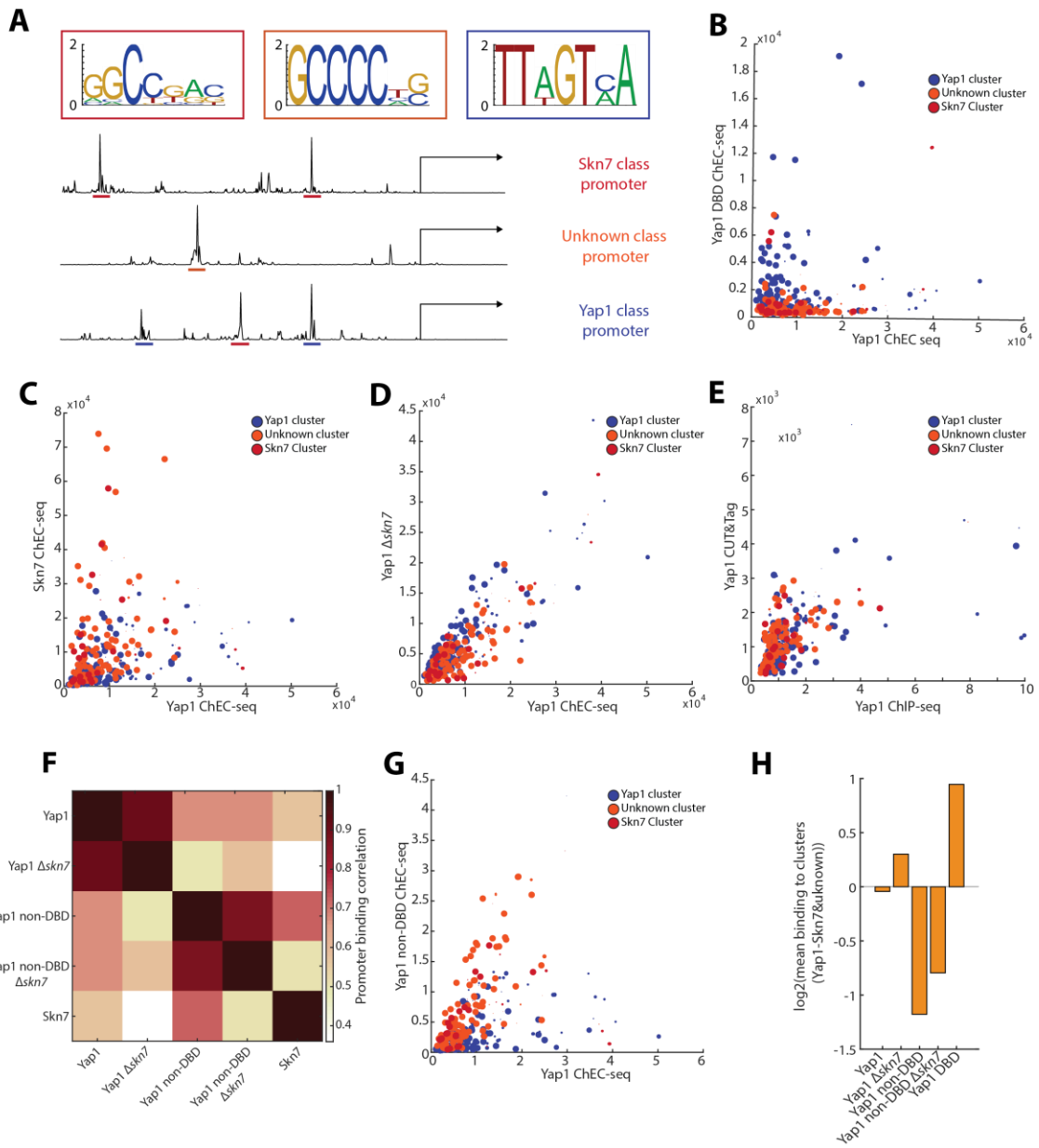

Figure SN5: Yap1 localization within promoters – distinct contributions of the DBD and of Skn7.

(A) *Three promoter classes defined by sequence motifs enriched in Yap1 binding sites:* Shown on top are the three PWM clusters, summarizing motif enrichment within Yap1-bound sites (See Methods section of the main text). Two of these consensus motifs correspond to the known Yap1 and Skn7 *in-vitro* preferences, while the third is unknown. Promoters were classified based on the occurrence of the associated 7-mers within Yap1 binding peaks, as shown (See Methods). A total of 345 promoters were assigned to one of the classes.

(B-C) *DBD-classified promoters are preferentially bound by the DBD-only mutant while promoters classified to the Skn7 or 'unknown' class are preferentially bound by Skn7:* Shown are the promoter binding strengths of the indicated TFs. Promoters are color-coded based on their classification, with classification confidence indicated by dot-size (See Methods).

(D) *Skn7 deletion causes a minor reduction of the Yap1 binding to promoters of the Skn7 and 'unknown' classes:* Shown are the promoter binding strength of Yap1 and Skn7, presentations as in (B-C).

(E) *ChIP-seq and CUT&Tag Yap1 profiling detects promoters of all classes:* Shown is the Yap1 promoter binding in the indicated profiles. Colors and sizes as in B-D.

(F) *Skn7 deletion reduces, but does not abolish, the high similarity between the non-DBD and Skn7 promoter binding:* Shown are the correlations in promoter selection of the indicated datasets.

(G) *Yap1 non-DBD shows reduced binding of DBD-classified promoters:* Same presentation as in (B-E).

(H) *Skn7 deletion partially rescues the reduced preference of the Yap1 non-DBD to DBD-classified promoters:* Shown is the log-ratio of binding strength between the Yap1-classified and Skn7/Unkown-classified promoters in the indicated datasets.

Conclusions:

Taken together, in the analysis presented in this supplementary note we validated the ChEC-seq binding profiles of Msn2, Yap1 and their mutants. This was done by (1) comparing those profiles to profiles generated by the two additional methods (ChIP-seq and CUT&Tag), (2) examining localization to known DNA binding motifs, and (3) assessing preferential binding of regulated promoters. First, we show that the two key binding profiles of our analysis: that of the intact TFs and that of their non-DBDs, are supported by two alternative binding methods and by gene expression data. Second, we conclude that only ChEC-seq, but neither of the other methods, can detect the binding profiles of the DBD and non-DBD mutants. These results provide support to our model presented in the main text and emphasize the need for using high-sensitivity methods for studying the principles of transcriptional regulation.

SUPLLEMENTAL NOTE METHODS

ChEC-seq experiments and analysis

All details regarding ChEC-seq experiments and analysis can be found in the Methods section of the main text.

Strains for ChIP-seq and CUT&Tag

To generate strains for ChIP-seq and CUT&Tag, TFs were C-terminally tagged with a 6HA tag, using the pYM17 plasmid (Janke et al., 2004). The transformation procedure is described in the Methods section of the main text. Strain information and oligos can be found in tables S2 and S3 of the main text.

CUT&Tag

The method that was developed by Kaya-Okur et al., 2019. for human cells was adjusted to yeast cells. As a preliminary step, yeast spheroplast were generated as previously described, excluding the Ficoll wash step (Kasinathan et al., 2014). Briefly, cells were grown in SD media to reach OD_{600} = 4. For each sample 2.5 ml culture were harvested by 2 minutes 2,700 g centrifugation at 4°C, followed by a cold-water wash and another centrifugation. Cells were resuspended in 500 µL of cold water, moved to 2 ml Low-bind tubes (Eppendorf 022431048) and pelleted at 2,700 g, 4°C for 5 minutes. Cells were resuspended in 50 µL of Resuspension Buffer (1.2 M sorbitol, 100 mM potassium phosphate pH 7.5, 0.5 M $CaCl_2$, and 0.5 mM β-mercaptoethanol) and incubated for 10 minutes at 37°C. Cells were supplemented with 0.1 mg Zymolase 10 mg/ml (Amsbio) and incubated for 15 minutes at 37°C. Cells were centrifuged at 1000 g in 4°C for 5 min, and washed twice with 1 ml of cold SPC buffer (1 M sorbitol, 200 mM PIPES, pH 6.3, 0.1 mM CaCl2, 1 mM PMSF and 50 µL protease inhibitor cocktail). Given the sensitivity of yeast spheroplasts to burst, all buffers were supplemented with 0.8 M sorbitol and resuspended by low-speed vortex from this step through to DNA extraction. Spheroplasts were resuspended in 500 µL Wash Buffer (20 mM HEPES pH 7.5, 150 mM NaCl, 0.5 mM spermidine, 1 × Roche cOmplete EDTA free protease inhibitors, 0.8 M sorbitol), pelleted at 600 g, room temperature (RT) for 3 minutes and resuspended in 100 µL Wash buffer. Concanavalin A coated magnetic beads (Bangs Laboratories) were prepared as described (Kaya-Okur et al., 2019), and 30 µL of activated beads were added dropwise to each sample while gently vortexing. Spheroplasts were incubated with beads for 15 minutes at RT on an end-over-end rotator. Next, samples were placed on a magnet stand and the

liquid was removed. Beads were resuspended in cold 50 µL Dig-wash Buffer (20 mM HEPES pH 7.5, 150 mM NaCl, 0.5 mM Spermidine, 1x Roche cOmplete EDTA free protease inhibitors, 0.8 M sorbitol, 0.05% Digitonin) containing 2 mM EDTA, 0.01% BSA and 1:50 primary antibody (12CA5 anti HA from hybridoma cells produced by the Antibody Unit at the Weizmann Institute). Overnight incubation was performed on a rotator at 4°C. Tubes were placed on a magnet stand and clear supernatant was removed. Beads were resuspended in 100 µL of Dig-wash Buffer containing 1:100 secondary antibody (Jackson Immunoresearch; 1.8 mg/ml stock) and incubated for 1-hour at RT on a rotator. Samples were placed on a magnet stand, supernatant was removed, and magnetized beads were washed twice with 1 ml Dig-wash Buffer. Beads were resuspended in 100 µL of Dig-150 Buffer (0.05% Digitonin, 20 mM HEPES, pH 7.5, 150 mM NaCl, 0.5 mM Spermidine, 0.8 M sorbitol, 1x Roche cOmplete EDTA free protease inhibitors) containing pA-Tn5 adapter complex (0.094 uM; in-house produced). Samples were incubated for 1-hour at RT on a rotator and then placed on a magnet to remove supernatant. Samples were washed twice with 1 ml Dig-150 Buffer using a magnet. Beads were resuspended in 300 µL Tagmentation Buffer (10 mM $MgCl_2$ in Dig-150 Buffer) and samples were incubated at 37°C for 1-hour. The reaction was stopped using 10 µL of 0.5 M EDTA, 3 µL of 10% SDS and 2.5 µL of 20 mg/mL Proteinase K (SigmaP2308). Samples were mixed by maximal speed vortex and incubated at 50°C overnight. 300 µL of Phenol chloroform were added to each sample, and tubes were vortexed and centrifuged 3 minutes at maximal speed. Then, 300 µL of chloroform were added, followed by another round of vortex and centrifugation. The aqueous layer was transferred to a new 1.5 ml Low-bind tube (Eppendorf 022431021) containing 750 µL of cold 96% ethanol. Samples were mixed by pipetting and incubated ~10 minutes on ice and then centrifuged at maximal speed for 15 minutes in 4°C. The supernatant was removed and DNA pellets were washed with 1 ml 96% cold ethanol. After removing the ethanol and allowing it to fully evaporate (~10 minutes), samples were treated for 20 minutes in 37°C with 2 µg RNase-A (Sigma, R4875) diluted in 25 µL 1X TE. To enrich for Tn5-cleaved DNA, the liquid of a reverse 0.5X SPRI (12.5 µL SPRI were added to 25 sample) clean-up was taken and resuspended in 1.8X SPRI cleanup with 2-propanol (32.5 µL SPRI beads and 135 µL 2-propanol were added to 37.5 sample). Library preparation was done as published, using KAPA HiFi HotStart ReadyMix (Kapa Biosystems). 1.1X SPRI cleanup was carried out on the final library. Libraries were then pooled and sequenced using Illumina NovaSeq6000 for paired end (50 bps for read1 and 50 bps for read 2). The number of repeats for each strain is indicated in Table S2.

ChIP-seq

The protocol used is a combination of the previously published SLIM-ChIP protocol and the ChIPmentation protocol (Gutin et al., 2018; Schmidl et al., 2015). Briefly, yeast cells were grown in SD media to reach OD_{600} = 4, then 12 ml culture were mixed with Formaldehyde to a final concentration of 1%. After 15 minutes incubation at RT, Glycine was added to a final concentration of 0.125 M for 5 minutes at RT. From this step on, cells were kept on ice. Cells were pelleted at 2,700 g, 4°C for 2 minutes and washed twice in 15 ml cold water. Samples were flash frozen in liquid nitrogen and stored at -80 °C. Cells were washed in 15 ml of cold 1 M sorbitol and pelleted by centrifugation (4000g, 2 minutes, 4°C). Pellets were resuspended in Buffer Z (1 M sorbitol, 50 mM Tris 7.4, 10 mM β-mercaptoethanol ; 5ul per 1 OD_{600}), treated with Zymolyase 10 mg /ml (Amsbio; 0.15 - 0.5 units per $2x10^7$ cells), and incubated for 30 minutes at 30°C. Spheroplasts were pelleted (6500 g, 5 minutes, 4°C) and resuspended in NP Buffer (10 mM Tris pH 7.4, 50 mM NaCl, 5 mM MgCl2, 1 mM CaCl2, and 0.075% NP-40, 1 mM β-mercaptoethanol, 500 µM spermidine, and 1X EDTA-free protease inhibitor cocktail; 5ul per 1 OD_{600}). Nuclei were pelleted (13.0k g, 10 minutes 4°C), and resuspended 100 µL of NP Buffer. Samples were sonicated

(Diagenode Bioruptor plus, 23 cycles, 30 on 30 off at high intensity). Lysate was transferred to 1.5 ml Low bind tubes (Eppendorf 022431021) containing 40 µL NP Buffer and vortexed 3 x 10 seconds. Samples were kept on ice for 30 minutes, vortexed an additional 3 x 10 seconds and centrifuged (16,000 g, 10 minutes, 4°C). Supernatant was transferred to fresh 96 well plate. 3 ug antibody (12CA5 anti HA from hybridoma cells produced by the Antibody Unit at the Weizmann Institute) were added to each sample, and samples were incubated 2.5 hours at 4°C. 20 µL of prewashed (3 washes in RIPA Buffer: 10 mM Tris pH 8.0, 140 mM NaCl, 1 mM EDTA, 0.1% SDS, 0.1% sodium deoxycholate, 1% Triton X-100, EDTA-free protease inhibitor cocktail) protein G Dynabeads (Invitrogen) were added to each sample and samples were incubated for 1 hour on a rotator at 4°C. The plate was placed on a magnetic stand and washed (150 µL per wash) 6 times with RIPA Buffer, 3 times with RIPA 500 (RIPA Buffer containing 500 mM NaCl), 3 times with LiCl wash buffer (10 mM Tris pH 8.0, 0.25 M LiCl, 0.5% NP-40, 0.5% Sodium Deoxycholate, 1 mM EDTA, 1X EDTA-free protease inhibitor cocktail), 3 times with 10 mM Tris pH 7.5. After the second Tris wash, the beads were transferred to new wells, and washed once with 10 mM Tris pH 8. Beads were resuspended with 15 µL of tagmentation reaction mix (7.5 µL 2xTD Buffer, 7.25 H2O, 0.25 µL Tn5 enzyme in-house produced as published), and incubated for 10 minutes at 37°C. The reaction was stopped by moving samples to ice and adding 140 µL RIPA Buffer (without protease inhibitors) per sample. Samples were washed 3 times on a magnetic stand with 150 µL RIPA buffer. Beads resuspended in 24 chromatin elution buffer (10 mM Tris pH 8.0, 5 mM EDTA, 300 mM NaCl, 0.6% SDS) supplemented with 1µl of 0.5 µg/µl RNase A (Sigma, R4875) were incubated for 30 minutes at 37°C. 22.5 µl of chromatin elution buffer supplemented with 2.5 µl of proteinase K (20 units/µl) were added to each sample for an additional 2 hours at 37°C, followed by 12-16 hours at 65°C. 2.2X SPRI beads cleanup was performed and DNA was eluted in 12µl of 10mM Tris pH-8.0. Sample were mixed with 1 µL of barcoded Tn5 primers and added to an activated 2X Kapa Hifi hotstart mix. DNA was amplified (5' 72°C, (98°C:20'', 63°C:20'' ,72°C:45'')x14, 5' 72°C). Finally, 1X SPRI beads cleanup was performed. Libraries were then pooled and sequenced using Illumina NovaSeq6000 for paired end (50 bps for read1 and 50 bps for read 2).

ChIP-seq and CUT&Tag processing and analysis

Paired end reads were aligned using bowtie 2 (parameters: "--very-sensitive --trim-to 40 --end-to-end") to *S. cerevisiae* (reference genome, cerR64). ChIP-seq and CUT&Tag tracks, representing the binding of each TF, were calculated by adding +1 to the 30 bps surrounding the middle of each read. The signal of each sample was then normalized to 10 million reads. Next steps of the analysis were performed exactly as for ChEC-seq (See main text Methods section).

Expression target definition

Expression targets of Msn2 were defined based on Chapal et al., 2019. The data includes time-resolved, genome-wide transcription profiling of wild-type cells and cells deleted of Msn2 (and its duplicate Msn4) that were subjected to a variety of stresses. Chosen experiments used for this analysis are termed: NaCL 0.4M, H2O2 0.3mM #1, H2O2 0.3mM #2, Heat shock #1 and Heat shock #2 in the original paper. First, 50-bp reads were mapped to the S. cerevisiae genome (reference genome, cerR64) using bowtie (parameters:–best -a -m 2 -strata -5 10). Then, reads for each sample were normalized to 1 million to account for sequence depth and log2 transformed. Next, genes that did not pass the threshold of 6 (log2 values) in 70% of time-points in all 6 experiments were filtered out. For each gene, we looked for the maximal fold change in the first 30 minutes of each experiment in order to focus on direct activation. Genes with median fold change > 1.4 were defined as Msn2 targets (72 genes in total). For Yap1, we used the set of targets defined by Tan et al. in both MMS and CDDP stresses (149 genes in total; Tan et al., 2008).

External binding data processing

Sequencing data from Kuang et al. was aligned and processed as described in the Methods section "ChEC-seq processing and analysis" of the main text (Kuang et al., 2017). The 3 samples of Msn2 from the reductive charging (RC) time points were averaged and used to compare promoter binding. Data from Harbison et al. - Log ratios of promoter binding from all samples in the different conditions of Msn2/Yap1 were averaged and used in the analysis (Harbison et al., 2004). Data from Venters et al. – log-ratios for each gene over both "UAS" and "TSS" were averaged followed by averaging of all Yap1 samples (25C and 37C; Venters et al., 2011). Data from Zentner et al. – BedGraph files were parsed and reads were normalized to 10 million, and the 3 repeats of Reb1 under 30 seconds calcium treatment were averaged and processed as in ChEC-seq processing and analysis (Zentner et al., 2015). Data from Tan et al. – All samples of Yap1 ChIP-chip were used, and annotations were converted to the new *S. cerevisiae* genome (reference genome, cerR64) using Lift Genome Annotations (Hinrichs, 2006; Tan et al., 2008). Genomic tracks were generated by assigning the log-ratio of a given tile to the 60 bps it corresponds to. Log-ratios for all annotated promoters were then calculated as for ChEC-seq. Median log ratio on each promoter over all samples was used in the analysis.

Motif enrichment within promoters

To define enrichment of motifs within promoters (Figure SN3C), the top 100 bound promoters by each TF were considered. The number of occurrences of each 5-mer in a combined sequence of those promoters was counted and normalized as follows:

$$\frac{Number\ of\ occurrences\ in\ \boldsymbol{top}\ promoters}{Number\ of\ occurrences\ in\ \boldsymbol{all}\ promoters} \times Number\ of\ all\ annotated\ promoters\ (5541).$$

Yap1/Skn7 promoter class definition

The median track of the Yap1 ChEC-seq profiles was used. For each annotated promoter, peaks (defined in Peak calling as described below) were called. For a given promoter, the number of occurrences of 7-mers from each of the 3 clusters (composing the PWMs shown in Figure S6I of the main text) in the 30 bps surrounding each peak was counted. Next, for each cluster, the number of occurrences in each promoter was normalized by the size of the cluster (cluster sizes: "Yap1" – 9, "Unknown – 22", "Skn7 – 16). Promoters were assigned to a given class based on the cluster that got the highest score. A confidence score (indicated by dot size in Figures SN5B-E & SN5G) was given based on the difference between the two top scoring clusters in each promoter. Promoters with values>0 in only one cluster were given a maximal confidence score.

Peak calling

Peak positions in our data were defined using a matlab function called "peakfinder" developed by Nathanael Yoder (parameters: sel=20,thresh=100).

References

Chapal, M., Mintzer, S., Brodsky, S., Carmi, M., and Barkai, N. (2019). Resolving noise-control conflict by gene duplication. PLoS Biol. *17*, e3000289.

Gutin, J., Sadeh, R., Alajem, A., Ram, O., and Friedman Correspondence, N. (2018). Fine-Resolution Mapping of TF Binding and Chromatin Interactions Data and Software Availability GSE108948.

Harbison, C.T., Gordon, D.B., Lee, T.I., Rinaldi, N.J., Macisaac, K.D., Danford, T.W., Hannett, N.M., Tagne, J.-B., Reynolds, D.B., Yoo, J., et al. (2004). Transcriptional regulatory code of a eukaryotic genome. Nature *431*, 99–104.

Hinrichs, A.S. (2006). The UCSC Genome Browser Database: update 2006. Nucleic Acids Res. *34*, D590–D598.

Janke, C., Magiera, M.M., Rathfelder, N., Taxis, C., Reber, S., Maekawa, H., Moreno-Borchart, A., Doenges, G., Schwob, E., Schiebel, E., et al. (2004). A versatile toolbox for PCR-based tagging of yeast genes: New fluorescent proteins, more markers and promoter substitution cassettes. Yeast *21*, 947–962.

Kasinathan, S., Orsi, G.A., Zentner, G.E., Ahmad, K., and Henikoff, S. (2014). High-resolution mapping of transcription factor binding sites on native chromatin. Nat. Methods *11*, 203–209.

Kaya-Okur, H.S., Wu, S.J., Codomo, C.A., Pledger, E.S., Bryson, T.D., Henikoff, J.G., Ahmad, K., and Henikoff, S. (2019). CUT&Tag for efficient epigenomic profiling of small samples and single cells. Nat. Commun. *10*, 1–10.

Kuang, Z., Pinglay, S., Ji, H., and Boeke, J.D. (2017). Msn2/4 regulate expression of glycolytic enzymes and control transition from quiescence to growth. Elife *6*.

Schmidl, C., Rendeiro, A.F., Sheffield, N.C., and Bock, C. (2015). ChIPmentation: Fast, robust, low-input ChIP-seq for histones and transcription factors. Nat. Methods *12*, 963–965.

Tan, K., Feizi, H., Luo, C., Fan, S.H., Ravasi, T., and Ideker, T.G. (2008). A systems approach to delineate functions of paralogous transcription factors: Role of the Yap family in the DNA damage response. Proc. Natl. Acad. Sci. U. S. A. *105*, 2934–2939.

Venters, B.J., Wachi, S., Mavrich, T.N., Andersen, B.E., Jena, P., Sinnamon, A.J., Jain, P., Rolleri, N.S., Jiang, C., Hemeryck-Walsh, C., et al. (2011). A Comprehensive Genomic Binding Map of Gene and Chromatin Regulatory Proteins in Saccharomyces. Mol. Cell *41*, 480–492.

Zentner, G.E., Kasinathan, S., Xin, B., Rohs, R., and Henikoff, S. (2015). ChEC-seq kinetics discriminates transcription factor binding sites by DNA sequence and shape in vivo. Nat. Commun. *6*, 8733.